

# Transition to an optimal periodic gait by simultaneous input and parameter optimization method of Hamiltonian systems

Satoshi Satoh · Kenji Fujimoto · Masami Saeki

Received: date / Accepted: date

**Abstract** This paper is concerned with a gait transition to an optimal periodic gait by a simultaneous input and parameter optimization technique of Hamiltonian systems. First, a continuous-time dynamics of a passive walking/running robot between the touchdown and lift-off is considered as a Hamiltonian system. Then, the control input and some robot parameters, such as the mass, inertia, link length and so on, are optimized by using learning optimal control of Hamiltonian systems, which has been developed by the authors. This method allows one to simultaneously obtain an optimal feed-forward input and optimal parameters, which (at least locally) minimize a given cost function. The main advantage is that the precise model of the dynamics of the plant system is not required by using a symmetric property of Hamiltonian systems, called variational symmetry. We formulate an optimal gait generation scheme via the learning optimal control, where the robot keeps walking and the gait is optimized with respect to the control input and some adjustable robot parameters si-

multaneously. As a result, the gait transition to an optimal periodic one is achieved.

**Keywords** Optimal control · Learning control · Robot control · Hamiltonian systems · Gait generation

## 1 Introduction

As technology for walking robots evolves, optimal gait generation and trajectory optimization schemes with respect to energy consumption become increasingly important. In this point of view, passive walking/running robot may suggest an ultimate energy-efficient gait. The passive walking robot was first studied in an engineering manner by McGeer [15]. This robot walks down a gentle slope powered only by gravity without any control input, and it exhibits a stable periodic gait under an appropriate initial condition. There have been various researches related to the passive walking such as stability analysis, e.g., [8, 16, 17], and limit cycle walking controllers based on the passive walking, e.g., [9, 22, 3, 2]. Besides, the passive running robot is a spring-driven one-legged hopping robot. The literature [23] shows that this robot has a special periodic running gait without any control input under appropriate initial condition. Since this periodic gait is unstable, several stabilization methods have been proposed, e.g., [1, 23], [13]. The main purpose of this paper is to achieve the gait transition to an optimal periodic gait with respect to the energy consumption such as a passive walking/running gait by applying a learning optimal control method of Hamiltonian systems.

The authors have been developing learning optimal control framework based on a symmetric property of Hamiltonian systems called variational symmetry [7, 5, 18, 20]. This method solves a class of optimal control

---

This work was partially supported by JSPS Grant-in-Aid for Young Scientists (B) (No. 15K18089).

S. Satoh  
Hiroshima University, 1-4-1 Kagamiyama, Higashi-Hiroshima  
739-8527, Japan  
E-mail: s.satoh@ieee.org

K. Fujimoto  
Kyoto University, Yoshida-Honmachi, Sakyo-ku, Kyoto 606-  
8501, Japan  
E-mail: fujimoto@kuaero.kyoto-u.ac.jp

M. Saeki  
Hiroshima University, 1-4-1 Kagamiyama, Higashi-Hiroshima  
739-8527, Japan  
E-mail: saeki@hiroshima-u.ac.jp

problems by iteration of laboratory experiments. The distinguished feature is that this method does not require the precise model of the dynamics of the plant system. Instead, it utilizes a universal property of Hamiltonian systems. So far, there are two types of learning methods based on the variational symmetry. One is iterative learning control (ILC) proposed in [7] and the other is iterative feedback tuning (IFT) proposed in [5]. For a given cost function, ILC is to optimize the feedforward control input, while IFT is to optimize the adjustable parameters. Both iteration laws of ILC and IFT are based on the steepest descent method, and the variational symmetry enables to approximately calculate the gradient of the cost function by the input-output map of the plant system, which can be obtained by laboratory experiments. Besides, the literature [20, 21] extends the basic idea of those ILC and IFT. In [20], a unified learning method of ILC and IFT has proposed, where optimal feedforward input and adjustable parameters minimizing a given cost function are simultaneously obtained. Subsequently, the report [21] considers some parameters of the plant system included in the Hamiltonian to be adjustable, and optimizes those parameters within prescribed ranges by applying the input saturation technique of ILC [4] to virtual inputs induced from the robot parameters.

In this paper, we apply the learning method reported in [21] to the passive walking and running robots, and simultaneously optimize the control input and some robot parameters, such as the mass distribution, spring stiffness, and link length. Since the robot keeps walking and the gait is optimized with respect to the energy consumption, the gait transition to an optimal periodic one is eventually achieved.

## 2 Learning optimal control unifying input optimization and parameter tuning

This paper considers the following Hamiltonian system with adjustable parameters  $\Sigma^{x_{t^0}} : U \rightarrow Y : u \mapsto y$

$$\begin{cases} \dot{x} = (J - R) \frac{\partial H(x, u, \rho)}{\partial x}^\top, & x(t^0) = x_{t^0} \\ y = -\frac{\partial H(x, u, \rho)}{\partial u}^\top \end{cases}. \quad (1)$$

Here,  $x(t) \in \mathbb{R}^n$  denotes the state, and  $u \in U$  and  $y \in Y$  represent the input and the output, respectively, where Hilbert spaces  $U$  and  $Y$  are  $U, Y = L_2^m[t^0, t^1]$  on a finite time interval  $[t^0, t^1]$ . The structure matrix  $J \in \mathbb{R}^{n \times n}$  and the dissipation matrix  $R \in \mathbb{R}^{n \times n}$  are skew-symmetric and symmetric positive semi-definite, respectively.  $\rho \in \mathbb{R}^s$  denotes a set of adjustable param-

eters. Since the variational symmetry, which plays an important role in optimization, is induced in a particular input-output map of Hamiltonian system (1), we define a virtual input with respect to the adjustable parameter  $\rho$  according to the IFT method in [5]. Let us introduce the following Zero-th order hold operator  $\mathfrak{h}$ , which maps  $\rho \in \mathbb{R}^s$  to the virtual input  $u_\rho \in U_\rho = L_2^s[t^0, t^1]$  as

$$\begin{aligned} \mathfrak{h} : \mathbb{R}^s &\rightarrow L_2^s[t^0, t^1] : \\ u_\rho(t) &:= (\mathfrak{h}(\rho))(t) \equiv \rho, \forall t \in [t^0, t^1]. \end{aligned} \quad (2)$$

Then, a corresponding output  $y_\rho \in Y_\rho = L_2^s[t^0, t^1]$  is defined as

$$y_\rho := -\frac{\partial H(x, u, u_\rho)}{\partial u_\rho}^\top$$

so that the input-output map  $u_\rho \mapsto y_\rho$  has variational symmetry.

According to [20], we define an extended input-output map in order to simultaneously optimize both the control input and the adjustable parameter by learning optimal control based on variational symmetry. Let us define the extended input  $u_e$  by  $u_e := (u^\top, u_\rho^\top)^\top \in U_e := U \times U_\rho$ , the extended output  $y_e$  by  $y_e := (y^\top, y_\rho^\top)^\top \in Y_e := Y \times Y_\rho$  and Hamiltonian  $H_e$  by  $H_e(x, u_e) := H(x, u, u_\rho)$ . Then, we have the following extended system  $\Sigma_e^{x_{t^0}} : U_e \rightarrow Y_e : u_e \mapsto y_e$

$$\begin{cases} \dot{x} = (J - R) \frac{\partial H_e(x, u_e)}{\partial x}^\top, & x(t^0) = x_{t^0} \\ y_e = -\frac{\partial H_e(x, u_e)}{\partial u_e}^\top \end{cases}. \quad (3)$$

Furthermore, this paper considers input constraints. Although the literature [4] has considered such constraints, this method only deals with the input saturations in ILC method. On the contrary, the proposed method can deal with the constraints for both the input and the parameter optimizations by introducing the constraints to the extended system (3). We suppose that the input constraints characterized by

$$u_e = \alpha(\hat{u}_e), \quad (4)$$

where  $\hat{u}_e$  denotes the command input and  $u_e$  means the actual input to the system. The saturation function  $\alpha(\hat{u}_e) = (\alpha_u(\hat{u}), \alpha_\rho(\hat{u}_\rho))^\top$  is supposed to be differentiable and given. By assigning appropriate saturation functions, we can optimize the control input and plant parameters within the prescribed ranges. We will show some possibilities of the saturation function later.

We investigate the variational symmetry of the input-output map of  $\Sigma_e^{x_{t^0}}$  in (3). By using Theorem 1 and Remark 1 in [7], we can give the following proposition:

**Proposition 1** Consider the Hamiltonian system  $\Sigma_e^{x,t^0}$  in (3). Suppose that there exists a nonsingular matrix  $T \in \mathbb{R}^{n \times n}$  satisfying

$$J = -TJ T^{-1}, \quad R = TR T^{-1} \quad (5)$$

$$\frac{\partial^2 H_e(x, u_e)}{\partial(x, u_e)^2} = \begin{pmatrix} T & 0_{n \times (m+s)} \\ 0_{(m+s) \times n} & I_{m+s} \end{pmatrix} \times \frac{\partial^2 H_e(x, u_e)}{\partial(x, u_e)^2} \begin{pmatrix} T^{-1} & 0_{n \times (m+s)} \\ 0_{(m+s) \times n} & I_{m+s} \end{pmatrix}. \quad (6)$$

Here,  $I_i$  and  $0_{i \times j}$  represent the  $i \times i$  identity matrix and  $i \times j$  zero matrix, respectively. Suppose moreover that, for two inputs  $v_e, w_e \in U_e$ , the corresponding state trajectories  $\xi(t), \zeta(t) \in \mathbb{R}^n, t \in [t^0, t^1]$  satisfy

$$\mathcal{R} \left( \frac{\partial^2 H_e(x, u_e)}{\partial(x, u_e)^2} \Big|_{\substack{x=\xi \\ u_e=v_e}} \right) = \frac{\partial^2 H_e(x, u_e)}{\partial(x, u_e)^2} \Big|_{\substack{x=\zeta \\ u_e=w_e}}, \quad (7)$$

where  $\mathcal{R}$  represents the time-reversal operator on  $[t^0, t^1]$  defined by

$$(\mathcal{R}(u))(t) = u(t^1 - t + t^0), \quad \forall t \in [t^0, t^1]. \quad (8)$$

Then, the following relationship holds:

$$(\delta \Sigma_e^{\xi(t^0)}(v_e))^*(\cdot) = \mathcal{R}(\delta \Sigma_e^{\zeta(t^0)}(w_e))\mathcal{R}(\cdot), \quad (9)$$

where  $(\delta \Sigma_e^{x(t^0)}(u_e))(\cdot)$  denotes the variational system of  $\Sigma_e^{x(t^0)}(u_e)$ , which corresponds to the Fréchet derivative of  $\Sigma_e^{x(t^0)}(u_e)$ , and  $(\delta \Sigma_e^{x(t^0)}(u_e))^*(\cdot)$  denotes its adjoint system.

Under the conditions in Proposition 1, a state-space realization of the adjoint system coincides with a time-reversal version of that of the variational system. This property is called variational symmetry of Hamiltonian systems. By using the relation (9) resulting from the variational symmetry, we convert the output of the adjoint system to that of the corresponding variational one. Moreover, the output of the variational system can be calculated by a difference approximation. Consequently, the input-output map of the adjoint system is obtained by only using the input-output data of the plant system. This is a key technique of our learning framework based on variational symmetry.

When the state trajectory has a particular feature compatible with the variational symmetry, we can obtain a more convenient relation than (9).

*Remark 1* A state trajectory under which the configuration coordinate  $q$  and the phase coordinate  $\dot{q}$  satisfy

$$q(t) = q(t^1 - t + t^0) \quad (10)$$

$$\dot{q}(t) = -\dot{q}(t^1 - t + t^0), \quad \forall t \in [t^0, t^1] \quad (11)$$

represents a time-symmetric motion with respect to the middle point of time  $t = (t^0 + t^1)/2$ . We call the trajectory satisfying the conditions (10) and (11) symmetric trajectory. Suppose a state trajectory  $\xi$  corresponding to an input  $v_e$  is symmetric trajectory, then the condition (7) in Proposition 1 is satisfied with  $\zeta = \xi$  and  $w_e = v_e$ , and therefore (9) is reduced to

$$(\delta \Sigma_e^{\xi(t^0)}(v_e))^*(\cdot) = \mathcal{R}(\delta \Sigma_e^{\xi(t^0)}(v_e))\mathcal{R}(\cdot). \quad (12)$$

Now, we derive the iteration law for the learning optimal control based on the variational symmetry considering input constraints (4). We consider a cost function to be minimized as  $\Gamma_e(\hat{u}_e, y_e) : U_e \times Y_e \rightarrow \mathbb{R}$ . Since the derivation of the iteration law is formally same as in [20], we only describe its outline. This paper executes learning optimal control along symmetric trajectories mentioned in Remark 1. Hence, the derivation here uses the relation (12) instead of (9). From (2) and (12), the Fréchet derivative of the cost function is given by

$$\begin{aligned} \delta \Gamma_e(\hat{u}_e, y_e)(\delta \hat{u}_e, \delta y_e) &= \langle \partial_{\hat{u}_e} \Gamma_e(\hat{u}_e, y_e), \delta \hat{u}_e \rangle_{U_e} + \langle \partial_{y_e} \Gamma_e(\hat{u}_e, y_e), \delta y_e \rangle_{Y_e} \\ &= \left\langle \partial_{\hat{u}_e} \Gamma_e + \frac{\partial \alpha(\hat{u}_e)^\top}{\partial \hat{u}_e} (\delta \Sigma_e^{x,t^0}(u_e))^*(\partial_{y_e} \Gamma_e), \delta \hat{u}_e \right\rangle_{U_e} \\ &= \left\langle \begin{pmatrix} \text{id } 0 \\ 0 \mathfrak{h}^* \end{pmatrix} \left( \partial_{\hat{u}_e} \Gamma_e + \frac{\partial \alpha} \partial \hat{u}_e}^\top (\delta \Sigma_e^{x,t^0}(u_e))^*(\partial_{y_e} \Gamma_e) \right), \begin{pmatrix} \delta \hat{u} \\ d\hat{\rho} \end{pmatrix} \right\rangle_{U \times \mathbb{R}^s} \\ &= \left\langle \begin{pmatrix} \partial_{\hat{u}} \Gamma_e \\ \mathfrak{h}^*(\partial_{\hat{\rho}} \Gamma_e) \end{pmatrix} + \begin{pmatrix} \frac{\partial \alpha_u}{\partial \hat{u}}^\top & 0 \\ 0 & \mathfrak{h}^* \frac{\partial \alpha_\rho}{\partial \hat{\rho}}^\top \end{pmatrix} \mathcal{R}(\delta \Sigma_e^{x,t^0}(u_e)) \circ \mathcal{R}(\partial_{y_e} \Gamma_e), \begin{pmatrix} \delta \hat{u} \\ d\hat{\rho} \end{pmatrix} \right\rangle_{U \times \mathbb{R}^s} =: \left\langle \begin{pmatrix} \nabla_{\hat{u}} \Gamma_e \\ \nabla_{\hat{\rho}} \Gamma_e \end{pmatrix}, \begin{pmatrix} \delta \hat{u} \\ d\hat{\rho} \end{pmatrix} \right\rangle_{U \times \mathbb{R}^s}, \end{aligned} \quad (13)$$

where  $\text{id}$  denotes the identity mapping.  $\partial_{\hat{u}_e} \Gamma_e = (\partial_{\hat{u}} \Gamma_e, \partial_{\hat{\rho}} \Gamma_e)$  and  $\partial_{y_e} \Gamma_e = (\partial_{y_e} \Gamma_e, \partial_{y_\rho} \Gamma_e)$  represent the partial gradients of the cost function with respect to  $\hat{u}_e$  and  $y_e$ , respectively, and  $\nabla_{\hat{u}} \Gamma_e$  and  $\nabla_{\hat{\rho}} \Gamma_e$  represent the gradients of the cost function with respect to  $\hat{u}$  and  $\hat{\rho}$ , respectively.

Once these gradients are calculated, the iteration is obtained based on the steepest descent method as

$$\begin{aligned} \hat{u}_{(i+1)} &= \hat{u}_{(i)} - K_{u(i)} \nabla_{\hat{u}} \Gamma_{e(i)} \\ \hat{\rho}_{(i+1)} &= \hat{\rho}_{(i)} - K_{\rho(i)} \nabla_{\hat{\rho}} \Gamma_{e(i)}, \end{aligned} \quad (14)$$

where the subscript  $(i)$  denotes the  $i$ th iteration and  $K_{u(i)}$  and  $K_{\rho(i)}$  are appropriate positive definite matrices. However, calculation of the gradients  $\nabla_{\hat{u}} \Gamma_{e(i)}$  and  $\nabla_{\hat{\rho}} \Gamma_{e(i)}$  generally requires the precise knowledge of the plant system. Regarding this, we show an approximate

calculation of the gradients by using the variational symmetry. From the definition of the Fréchet derivative, the following approximation of the gradients in (13) holds with a sufficiently small constant  $\epsilon_e > 0$ :

$$\begin{aligned} \begin{pmatrix} \nabla_{\hat{u}} \Gamma_e \\ \nabla_{\hat{\rho}} \Gamma_e \end{pmatrix} &\approx \begin{pmatrix} \partial_{\hat{u}} \Gamma_e \\ \mathfrak{h}^*(\partial_{\hat{\rho}} \Gamma_e) \end{pmatrix} + \begin{pmatrix} \frac{\partial \alpha_u}{\partial \hat{u}} \top \mathcal{R} & 0 \\ 0 & \mathfrak{h}^* \frac{\partial \alpha_\rho}{\partial \hat{\rho}} \top \mathcal{R} \end{pmatrix} \\ &\times \left( \frac{\Sigma_e^{x_i^0}(u_e + \epsilon_e \mathcal{R}(\partial_{y_e} \Gamma_e)) - \Sigma_e^{x_i^0}(u_e)}{\epsilon_e} \right). \end{aligned} \quad (15)$$

Consequently, from (14) and (15), the iteration law for the learning optimal control is given by

$$\begin{cases} u_{(2i+1)} = u_{(2i)} + \epsilon_{e(i)} \mathcal{R}(\partial_{y_e} \Gamma_{e(2i)}) \\ u_{\rho(2i+1)} = \mathfrak{h}(\rho_{(2i)}) + \epsilon_{e(i)} \mathcal{R}(\partial_{y_\rho} \Gamma_{e(2i)}) \end{cases} \quad (16)$$

$$\begin{cases} \hat{u}_{(2i+2)} = \hat{u}_{(2i)} - K_{u(i)} \left( \partial_{\hat{u}} \Gamma_{e(2i)} + \frac{\partial \alpha_u(\hat{u}_{(2i)}) \top}{\partial \hat{u}} \frac{1}{\epsilon_{e(i)}} \mathcal{R}(y_{(2i+1)} - y_{(2i)}) \right) \\ \hat{\rho}_{(2i+2)} = \hat{\rho}_{(2i)} - K_{\rho(i)} \left( \int_{t^0}^{t^1} \partial_{\hat{\rho}} \Gamma_{e(2i)} + \frac{\partial \alpha_\rho(\hat{\rho}_{(2i)}) \top}{\partial \hat{\rho}} \frac{1}{\epsilon_{e(i)}} \mathcal{R}(y_{\rho(2i+1)} - y_{\rho(2i)}) dt \right). \end{cases} \quad (17)$$

Provided that the initial control input, parameter and initial condition are appropriately chosen, respectively. In the derivation of (17), we use the following fact:

**Lemma 1** [5] *For any  $\eta \in L_2^s[t^0, t^1]$ ,  $\mathfrak{h}^*$  is characterized by*

$$\mathfrak{h}^*(\eta) = \int_{t^0}^{t^1} \eta(t) dt.$$

The pair of iteration laws (16) and (17) implies that this learning procedure needs two steps laboratory experiments to execute a single update in the steepest decent method (14) due to the difference approximation of the variational system (15).

### 3 Application to the passive walking robot

This section considers the passive walking robot depicted in Fig. 1, left, and we apply the proposed learning method to this robot in order to generate a passive walking gait as an optimal solution.

We define the generalized coordinate  $q = (q_1, q_2)^\top \in \mathbb{R}^2$  as  $q := (\theta_1, \theta_2)^\top$ , where  $\theta_1$  and  $\theta_2$  denote the stance and swing angles, respectively. The state  $x := (q^\top, p^\top)^\top$ ,

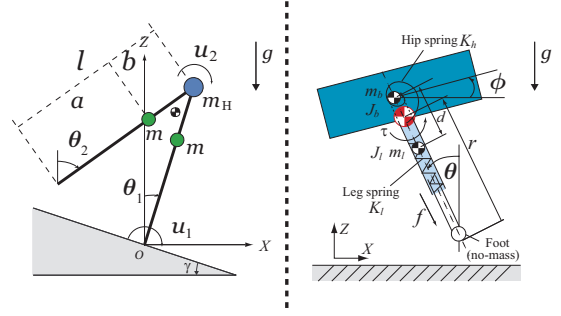


**Fig. 1** Passive walking and running robots

where the generalized momentum  $p \in \mathbb{R}^2$  is given by  $p = M(q)\dot{q}$  with an inertia matrix  $M(q)$ . The control input is denoted by  $u := (u_1, u_2)^\top \in \mathbb{R}^2$ , where  $u_1$  and  $u_2$  represent the ankle and hip torques, respectively. See [10], for the detail of the equation of motion of the robot.

In order to prevent the robot from falling during learning, we add a virtual potential energy  $P_c$  such as

$$P_c := \frac{k_c}{2}(q_1 + q_2)^2 \quad (18)$$

to restrict the motion of the robot to a symmetric trajectory satisfying  $q_1 + q_2 = 0$ . Here, the gain parameter  $k_c$  represents the constraint strength. We let  $k_c$  sufficiently large at the beginning of the learning steps, so that the robot is expected to avoid falling due to [14]. Compared to the conventional constraint methods with the output zeroing control [11,14], the advantages of this method are as follows. First, it does not require the model parameters of the plant system, since the potential energy (18) can be generated by a simple feedback controller

$$u = \bar{u} - k_c A_c q, \quad A_c := \begin{pmatrix} 1 & 1 \\ 1 & 1 \end{pmatrix}, \quad (19)$$

where  $\bar{u}$  denotes the learning input. Second, after adding the potential energy, the plant system preserves the Hamiltonian structure [6] and the constraint parameter  $k_c$  is explicitly contained in a new Hamiltonian.

Next, we suppose the mass distribution parameter  $b$  (see, Fig. 1) to be adjustable, which also appears in the Hamiltonian. Thus, we define the adjustable parameter vector as  $\rho := (k_c, b)^\top$ . Due to the definitions, both  $k_c \geq 0$  and  $0 \leq b \leq l$  should be satisfied. In order to optimize those parameters within the prescribed ranges, we equip the following constraint functions

$$F_1(v; \nu) := \begin{cases} 0 & (v < 0) \\ -\frac{v^3}{\nu^2} + \frac{2v^2}{\nu} & (0 \leq v < \nu) \\ v & (v \leq \nu) \end{cases} \quad (20)$$

$$F_2(v; \nu) := \frac{\nu}{2} \left( 1 + \tanh \left( \frac{2v - \nu}{\nu} \right) \right), \quad (21)$$

where a design parameter  $\nu$  is a positive constant. For simplicity, we do not consider the constraint on the learning input  $\bar{u}$  in this section. Then, we have the extended input as  $u_e = (\bar{u}^\top, u_\rho^\top)^\top$  with  $u_\rho := (\mathfrak{h}(k_c), \mathfrak{h}(b))^\top$ , and define the saturation function

$$\bar{u} = \alpha_u(\hat{u}) = \hat{u}$$

$$u_\rho = \alpha_\rho(\hat{u}_\rho) = (F_1(\hat{u}_{\rho,1}; \nu), F_2(\hat{u}_{\rho,2}; l))^\top.$$

According to the definition of the output, we have  $y_e = (y^\top, y_\rho^\top)^\top$  with  $y = q$  and

$$y_{\rho,1} = -\frac{(q_1 + q_2)^2}{2}$$

$$y_{\rho,2} = -m(l-b)\dot{q}_1^2 + mb\dot{q}_2^2 - ml \cos(q_1 - q_2)\dot{q}_1\dot{q}_2 + mg(\cos q_1 + \cos q_2).$$

Now, we propose a cost function as

$$\begin{aligned} \Gamma_e(\hat{u}_e, y_e) := & \quad (22) \\ & \frac{1}{2} \int_{t^0}^{t^1} (y(\tau) - C\mathcal{R}(y)(\tau))^\top \lambda(\tau) A_y (y(\tau) - C\mathcal{R}(y)(\tau)) d\tau \\ & + \frac{1}{2} \int_{t^0}^{t^1} (\hat{u}(\tau)^\top A_{\bar{u}} \hat{u}(\tau) + \hat{u}_\rho(\tau)^\top A_\rho \hat{u}_\rho(\tau)) d\tau, \end{aligned}$$

where appropriate positive definite matrices  $A_y$ ,  $A_{\bar{u}}$ ,  $A_\rho \in \mathbb{R}^{2 \times 2}$  represent weight matrices, respectively. The matrix  $C$  exchanges the support and swing leg angles, and is given by

$$C = \begin{pmatrix} 0 & 1 \\ 1 & 0 \end{pmatrix},$$

and  $\lambda(t) \in \mathbb{R}$  denotes the filter function defined by

$$\lambda(t) := \begin{cases} \frac{1}{2} \left( 1 - \cos\left(\frac{t^0 + \Delta t - t}{\Delta t} \pi\right) \right) & (t^0 \leq t \leq t^0 + \Delta t) \\ 0 & (t^0 + \Delta t < t \leq t^1) \end{cases},$$

where a design parameter  $\Delta t$  is a positive constant. The first term of the cost function (22) is a necessary condition for a periodic trajectory such that  $q_1(t^0) \equiv q_2(t^1)$  and  $q_2(t^0) \equiv q_1(t^1)$ . The second term is to minimize the learning input. The last term is to mitigate the strength of the virtual constraint, and to optimize the robot parameter. Let us note that although another necessary condition with respect to  $\dot{q}$  can be utilized as in [19], where initial angular velocities are equivalent to velocities just after touch down. However, it is not equipped here for simplicity of iteration law. From (16) and (17), we obtain the iteration law as

$$\begin{cases} \hat{u}_{(2i+1)} = \hat{u}_{(2i)} + \epsilon_{e(i)} \mathcal{R} \left( (\text{id} - \mathcal{R}C) \lambda A_y \right. \\ \quad \left. \times (\text{id} - \mathcal{R}) (y_{(2i)}) \right) \\ \hat{\rho}_{(2i+1)} = \hat{\rho}_{(2i)} \end{cases} \quad (23)$$

$$\begin{cases} \hat{u}_{(2i+2)} = \hat{u}_{(2i)} - K_{u(i)} \left( A_{\bar{u}} \hat{u}_{(2i)} \right. \\ \quad \left. + \frac{1}{\epsilon_{e(i)}} \mathcal{R}(y_{(2i+1)} - y_{(2i)}) \right) \\ \hat{\rho}_{(2i+2)} = \hat{\rho}_{(2i)} - K_{\rho(i)} \left( \int_{t^0}^{t^1} A_\rho \hat{u}_{\rho(2i)} + \frac{1}{\epsilon_{e(i)}} \right. \\ \quad \left. \times \begin{pmatrix} \frac{\partial F_1(\hat{u}_{\rho,1})}{\partial \hat{u}_{\rho,1}} & 0 \\ 0 & \frac{\partial F_2(\hat{u}_{\rho,2})}{\partial \hat{u}_{\rho,2}} \end{pmatrix}^\top \mathcal{R}(y_{\rho(2i+1)} - y_{\rho(2i)}) dt \right). \end{cases} \quad (24)$$

Here,  $[t^0, t^1]$  denotes a predetermined cycle of periodic walking, which is estimated by the free motion under the initial condition. In the following simulations, if  $i$ th cycle is longer than this, the excess time-series data is truncated. If it is shorter than this, the last data is repeatedly used until the terminal time  $t^1$ .

We apply the learning procedure (23), (24) to the passive walking robot in Fig. 1, left. The ground inclination is set to  $\gamma = 0.05$  rad. The physical parameters of the robot are chosen as  $m_H = 10$ ,  $m = 5$  kg and  $l = 1.0$  m. We utilize the following design parameters with respect to the weighting functions for the cost function (22) as  $A_y = \text{diag}(0.5, 1)$ ,  $A_{\bar{u}} = \text{diag}(1, 1)$ ,  $A_\rho = \text{diag}(5, 2)$ , that with respect to the filter function as  $\Delta t = 1.0 \times 10^{-2}$  s, and those with respect to learning algorithm as  $K_{u(\cdot)} = \text{diag}(0.1, 0.1)$ ,  $K_{\rho(\cdot)} = \text{diag}(5.0 \times 10^{-3}, 1.0 \times 10^{-5})$  and  $\epsilon_{e(\cdot)} = 1$ . In this simulation, we proceed 500 steps of the learning procedure, which means the robot continued 1000 cycles of walking, with the initial condition  $(q_{1t^0}, q_{2t^0}, \dot{q}_{1t^0}, \dot{q}_{2t^0}) = (-0.24, 0.27, 1.2, 0.35)$  and with the zero initial learning input, that is,  $\hat{u}_{(0)} \equiv 0$ . The initial values of the adjustable parameters are chosen as  $k_{c(0)} = 5$  and  $b_{(0)} = 0.65$  m, where the total leg length  $l$  is fixed as  $l = 1$  m. The constraint functions in Eqs. (20) and (21) are used as  $F_1(\cdot; 0.25)$  and  $F_2(\cdot; 1)$ , respectively.

Figure 2 shows the history of the cost function (22) along the walking steps. Since the cost function monotonically decreases along the walking steps and then converges to a constant value, it implies that at least a local minimum of the cost function has been achieved smoothly. Figure 3 shows the histories of the constraint parameter  $k_c$  and robot parameter  $b$  along the walking steps. The upper figure implies that the strength of the virtual constraint automatically converges to zero according to the progress of learning, and the bottom figure exhibits that the mass distribution of the leg is adjusted. Figure 4 shows that the  $L_2$  norm of all the control input  $u$  in Eq. (19) converges to zero along the iteration. Figure 5 exhibits the phase portraits of  $q$ - $\dot{q}$ . The fact that a periodic trajectory is generated follows from that the phase portrait in the figure forms a closed orbit. From those figures, it is concluded that the gait

transition from an active walking to a passive one is eventually achieved as an optimal solution of the proposed learning method.

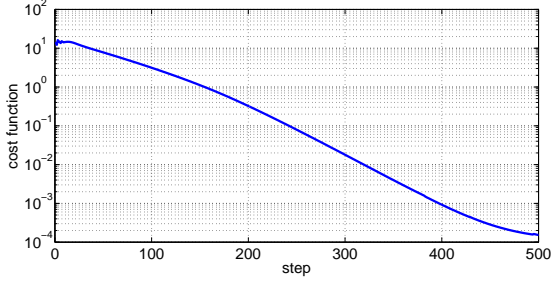


Fig. 2 Cost function

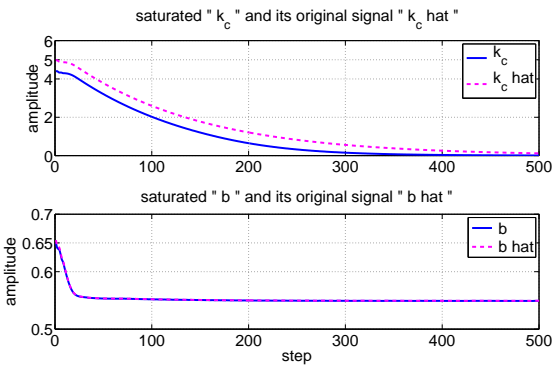


Fig. 3 Constraint parameter  $k_c$  and robot parameter  $b$

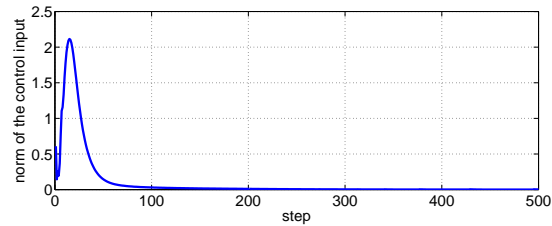


Fig. 4 Norm of all the control input  $u$

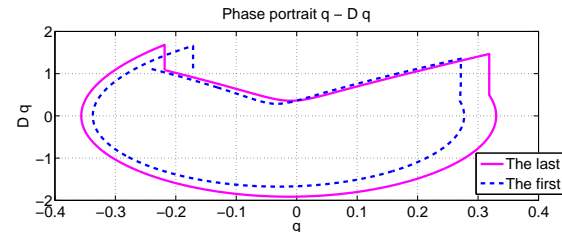


Fig. 5 Phase portraits with respect to  $q - \dot{q}$

## 4 Application to the passive running robot

This section applies the proposed method to the passive running robot depicted in Fig. 1, right in order to generate an optimal periodic running gait as an optimal solution. Table 1 shows the physical parameters.

Table 1 Parameters and variables

Notation	Meaning	Unit	Value
$m_b$	Body mass	kg	10
$m_l$	Leg mass	kg	2
$M$	Total mass ( $m_b + m_l$ )	kg	12
$J_b$	Body inertia	kgm <sup>2</sup>	0.50
$J_l$	Equivalent leg inertia	kgm <sup>2</sup>	0.11
$r_0$	Natural leg length	m	0.50
$g$	Gravity acceleration	m/s <sup>2</sup>	9.8
$K_l$	Leg spring stiffness	N/m	3000
$\phi$	Body angle	rad	
$\theta$	Leg angle	rad	
$r$	Leg length	m	
$X$	Horizontal CoM(*)	m	
$Z$	Vertical CoM(*)	m	
$\tau$	Hip torque	Nm	
$K_h$	Hip spring stiffness	Nm/rad	

(\*) CoM means the center of mass.

See [13] for the details. One locomotion cycle consists of the stance phase, where the leg touches the ground and the leg spring is compressed, and the flight phase, where the leg is above the ground and the robot traverses a ballistic trajectory. We assume that the foot does not bounce back nor slip on the ground. According to [13], the dynamics of this robot is described as

Stance phase :

$$\begin{aligned}
 M\ddot{r} + K_l(r - r_0) - Mr\dot{\theta}^2 &= Mg(1 - \cos\theta) + f \\
 (J_l + Mr^2)\ddot{\theta} + 2Mr\dot{r}\dot{\theta} - K_h(\phi - \theta) &= rMg\sin\theta - \tau \\
 J_b\ddot{\phi} + K_h(\phi - \theta) &= \tau
 \end{aligned} \tag{25}$$

Flight phase :

$$\begin{aligned}
 \ddot{X} &= 0 \\
 \ddot{Z} &= -g \\
 J_l\ddot{\theta} + J_b\ddot{\phi} &= 0 \\
 J_b\ddot{\phi} + K_h(\phi - \theta) &= \tau.
 \end{aligned} \tag{26}$$

During the running, energy dissipation generally occurs at the touchdown. The literature [13] gives the variation of the energy between just before and after the touchdown denoted by  $\Delta E$  can be calculated as

$$\Delta E = -\frac{MJ_l}{2(J_l + Mr_0^2)}(\mu^-)^2, \tag{27}$$

where the energy dissipation coefficient  $\mu^-$  is defined as

$$\mu^- := \dot{X}^- \cos \theta^- + \dot{Z}^- \sin \theta^- + r_0 \dot{\theta}^-. \quad (28)$$

Here,  $\dot{X}^-$ ,  $\dot{Z}^-$ ,  $\dot{\theta}^-$  represent the velocity of the center of mass and the angular velocity just before touchdown, respectively. From (27) and (28), the condition

$$\mu^- = 0 \quad (29)$$

implies  $\Delta E = 0$  and it means that there is no energy transfer except for the control input. If the total mechanical energy is completely preserved, a periodic running gait is expected to be generated.

The leg angle  $\theta$  is the most important state variable in controlling running gait, because it has a direct effect to avoid falling. However, it is difficult to be controlled in the stance phase, since this robot has no foot and ankle torque is not available. Therefore, as in [12], we apply zero control input in the stance phase, i.e.,  $\tau = f = 0$  in (25), and try to control  $\theta$  in the flight phase by using the hip torque  $\tau$ . According to [1, 13], the synchronization of the body and leg oscillatory motions satisfying

$$J_l \theta(t) + J_b \phi(t) = 0 \quad (30)$$

is important for one-periodic passive running. From the dynamics (26), under the initial condition at the flight phase  $\theta(0)$ ,  $\dot{\theta}(0)$ ,  $\phi(0)$ ,  $\dot{\phi}(0)$  satisfying  $J_l \theta(0) + J_b \phi(0) = 0$  and  $J_l \dot{\theta}(0) + J_b \dot{\phi}(0) = 0$ , the synchronization (30) is achieved in the flight phase. Under the synchronization (30), we can extract the dynamics of  $\theta$  from the dynamics in (26) as

$$\begin{aligned} \begin{pmatrix} \dot{q} \\ \dot{p} \end{pmatrix} &= \begin{pmatrix} 0 & 1 \\ -1 & 0 \end{pmatrix} \begin{pmatrix} \frac{\partial H(q,p,u)}{\partial q} \\ \frac{\partial H(q,p,u)}{\partial p} \end{pmatrix} \\ H(q,p,u) &:= \frac{1}{2J_l} p^2 + \frac{1}{2} \frac{(J_b + J_l)}{J_b} K_h q^2 - qu, \\ y &= -\frac{\partial H(q,p,u)}{\partial u} = q = \theta \end{aligned} \quad (31)$$

where  $q := \theta$ ,  $p := J_l \dot{\theta}$  and we define the control input as  $u = -\tau$  in order to unify the resultant Hamiltonian representation with that in the literature [18–21].

In order to prevent the robot from falling during learning, we add the following feedback

$$u = \bar{u} - k_c \left( \theta + \frac{J_b}{J_l} \phi \right) - K_D \left( \dot{\theta} + \frac{J_b}{J_l} \dot{\phi} \right), \quad (32)$$

with  $\phi$  and  $\dot{\phi}$  considered to be reference signals for local PD feedback.  $\bar{u}$  denotes the learning input. The local PD feedback in (32) is expected to keep the synchronization (30). The gain parameter  $k_c$  represents the constraint strength, and we let  $k_c$  sufficiently large at the beginning of the learning, so that the robot is expected to avoid falling. The closed loop system by (32) becomes

again the Hamiltonian system, and moreover the constraint parameter  $k_c$  is explicitly contained in the new Hamiltonian.

Here, we suppose that the hip spring stiffness  $K_h$  to be adjustable, and define the adjustable parameter vector as  $\rho := (k_c, K_h)^\top$ . Then, we have the extended input as  $u_e = (\bar{u}, u_\rho^\top)^\top$  with  $u_\rho := (\mathfrak{h}(k_c), \mathfrak{h}(K_h))^\top$ . Consequently, the resultant dynamics of  $\theta$  under the synchronization with zero reference signals for the local PD feedback is given by

$$\begin{aligned} \begin{pmatrix} \dot{q} \\ \dot{p} \end{pmatrix} &= \begin{pmatrix} 0 & 1 \\ -1 & -K_D \end{pmatrix} \begin{pmatrix} \frac{\partial \bar{H}(q,p,\bar{u},u_\rho)}{\partial q} \\ \frac{\partial \bar{H}(q,p,\bar{u},u_\rho)}{\partial p} \end{pmatrix} \\ \bar{H}(q,p,\bar{u},u_\rho) &:= \frac{1}{2J_l} p^2 + \frac{1}{2} \left( u_{\rho,1} + \frac{(J_b + J_l)}{J_b} u_{\rho,2} \right) q^2 - q\bar{u} \\ y &= -\frac{\partial \bar{H}(q,p,\bar{u},u_\rho)}{\partial \bar{u}} = q = \theta \\ y_{\rho,1} &= -\frac{\partial \bar{H}(q,p,\bar{u},u_\rho)}{\partial u_{\rho,1}} = -\frac{1}{2} q^2 \\ y_{\rho,2} &= -\frac{\partial \bar{H}(q,p,\bar{u},u_\rho)}{\partial u_{\rho,2}} = -\frac{1}{2} \frac{(J_b + J_l)}{J_b} q^2 \end{aligned} \quad (33)$$

Due to the definitions, both  $k_c \geq 0$  and  $K_h \geq 0$  should be satisfied, and thus we define the saturation function  $\alpha_u(\hat{u}) = \hat{u}$  and  $\alpha_\rho(\hat{u}_\rho) = (F_1(\hat{u}_{\rho,1}; \nu), F_1(\hat{u}_{\rho,2}; \nu))^\top$ . For simplicity, we do not consider the constraint on  $\bar{u}$ .

The literature [13] shows that a symmetric trajectory satisfying (10) and (11) is a sufficient condition for (29), namely, for a periodic running gait. Moreover, as a special case, a symmetric trajectory with particular initial condition becomes a passive running gait, which satisfies (29) without the control input. In order to generate an optimal periodic gait, we equip a cost function which encourages to generate a symmetric trajectory without any reference trajectory, minimizes the control input  $u$  in (32) and optimizes the robot parameter  $K_h$ . Note that optimization of the robot parameter as well as minimization of the control input is very significant for generating a passive running gait. For this purpose, the literature [13] proposes a dead-beat control letting trajectory symmetric with extra adaptation scheme of  $K_h$ , and the literature [18] proposes an ILC method optimizing both the control input and the initial condition. This paper achieves this objective by using learning optimal control unifying input optimization and robot parameter tuning. Now, we propose a cost function as

$$\begin{aligned} \Gamma_e(\hat{u}_e, y_e) &:= \frac{\Lambda_y}{2} \int_{t^0}^{t^1} |y(\tau) + (\mathcal{R}(y))(\tau)|^2 d\tau \\ &+ \frac{\Lambda_{\bar{u}}}{2} \int_{t^0}^{t^1} |\hat{u}(\tau)|^2 d\tau + \frac{1}{2} \int_{t^0}^{t^1} \hat{u}_\rho(\tau)^\top \Lambda_\rho \hat{u}_\rho(\tau) d\tau, \end{aligned} \quad (34)$$

where  $\Lambda_y$  and  $\Lambda_{\bar{u}}$  represent appropriate positive constants, and  $\Lambda_\rho$  represent appropriate positive definite matrix, respectively.  $\mathcal{R}$  is the time-reversal operator as

defined in (8). The first term is a constraint letting the condition (10) for a symmetric trajectory be satisfied. For another condition (11), we can impose the constraint term with respect to  $\dot{y}$  as  $|\dot{y} - \mathcal{R}(\dot{y})|^2$  as reported in [18]. The proposed constraint terms with time-reversal operator do not need any reference trajectory to generate a symmetric trajectory. The second term in (34) minimizes the  $L_2$  norm of the learning input, and the last term optimizes the constraint and robot parameters. From (16) and (17), we obtain the iteration law as

$$\begin{cases} \hat{u}_{(2i+1)} = \hat{u}_{(2i)} + 2\epsilon_{e(i)} \mathcal{R}\left(A_y(\text{id} + \mathcal{R})(y_{(2i)})\right) \\ \hat{\rho}_{(2i+1)} = \hat{\rho}_{(2i)} \end{cases} \quad (35)$$

$$\begin{cases} \hat{u}_{(2i+2)} = \hat{u}_{(2i)} - K_{u(i)} \left( A_{\bar{u}} \hat{u}_{(2i)} + \frac{1}{\epsilon_{e(i)}} \mathcal{R}(y_{(2i+1)} - y_{(2i)}) \right) \\ \hat{\rho}_{(2i+2)} = \hat{\rho}_{(2i)} - K_{\rho(i)} \left( \int_{t^0}^{t^1} A_{\rho} \hat{u}_{\rho(2i)} + \frac{1}{\epsilon_{e(i)}} \right. \\ \left. \times \begin{pmatrix} \frac{\partial F_1(\hat{u}_{\rho,1})}{\partial \hat{u}_{\rho,1}} & 0 \\ 0 & \frac{\partial F_1(\hat{u}_{\rho,2})}{\partial \hat{u}_{\rho,2}} \end{pmatrix} \mathcal{R}(y_{\rho(2i+1)} - y_{\rho(2i)}) dt \right). \end{cases} \quad (36)$$

The D gain in the PD feedback (32) is updated according to the P gain, namely  $\rho_1 = k_c$  as  $K_{D(i)} = K_{D(0)} k_{c(i)} / k_{c(0)}$  in order to preserve the ratio of PD gains. Here,  $[t^0, t^1]$  denotes a predetermined flight phase, which is estimated by the free motion under the initial condition.

We exhibit the simulation results by applying the iteration law (35) and (36) to the passive running robot in Fig. 1, right. We proceed 50 steps of the learning procedure, which means the robot continued 100 cycles of running. We use the following design parameters:  $A_y = 0.3$ ,  $A_{\bar{u}} = 1 \times 10^{-5}$ ,  $A_{\rho} = \text{diag}\{1 \times 10^{-3}, 1 \times 10^{-3}\}$ ,  $K_{u(i)} = 1 \times 10^{-4}$ ,  $K_{\rho(i)} = \text{diag}\{3 \times 10^{-3}, 2 \times 10^{-3}\}$  and  $\epsilon_{e(i)} = 0.1$ . The saturation function is chosen as

$$\alpha_{\rho}(\hat{u}_{\rho}) = (F_1(\hat{u}_{\rho,1}; 0.25), F_1(\hat{u}_{\rho,2}; 0.25))^{\top}.$$

We start the running from the stance phase with the following initial condition:

$$\begin{aligned} (r(0), \theta(0), \phi(0), \dot{r}(0), \dot{\theta}(0), \dot{\phi}(0)) \\ = (0.5000, 0.3200, -0.0704, -2.4817, -2.5691, 0.5654). \end{aligned}$$

At flight phase, the initial learning input  $\hat{u}_{(0)} \equiv 0$  and the adjustable robot parameter  $K_{h(0)} = 10$  are utilized. Figure 6 shows the history of the cost function (34) along the running steps. Although it is not monotonic, the cost function decreases and eventually converges, which means at least a local minimum is achieved. The proposed method is based on the steepest

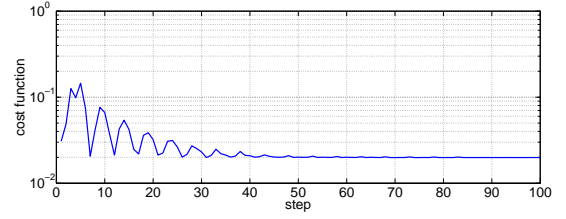


Fig. 6 Cost function

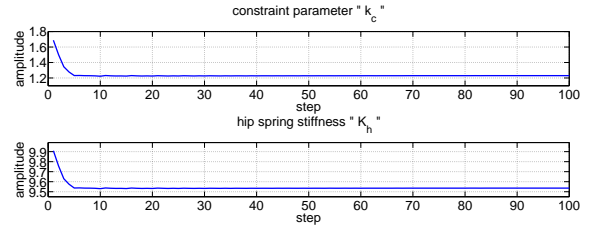


Fig. 7 Constraint parameter  $k_c$  and robot parameter  $K_h$

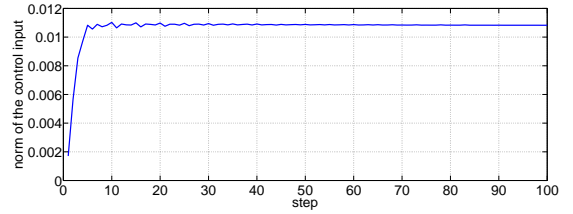


Fig. 8 Norm of all the control input  $u$

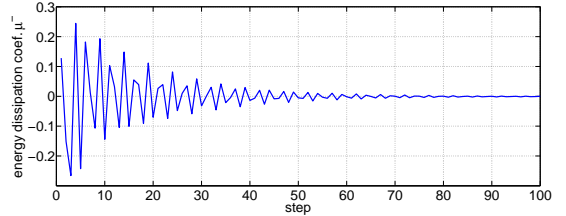


Fig. 9 Energy dissipation coefficient  $\mu^-$

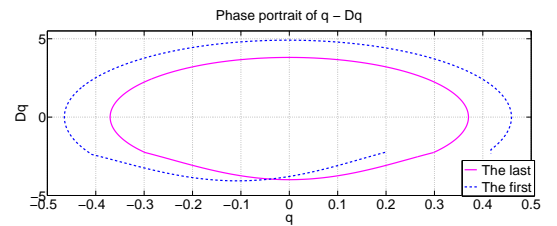


Fig. 10 Phase portraits with respect to  $q - \dot{q}$

descent method and this simulation uses fixed learning gains  $K_u$  and  $K_{\rho}$ . This may cause the transient fluctuation around the (local) minimum of the cost function. Figure 7 shows the histories of the constraint parameter  $k_c$  and robot parameter  $K_h$  along the running steps. The upper figure implies that the strength of the virtual constraint automatically mitigated according to



the progress of learning, and the bottom figure exhibits that the hip spring stiffness is adjusted by learning. Figure 8 exhibits  $L_2$  norm of all the control input  $\hat{u}$  in Eq. (32). From Fig. 8, although the resultant periodic gait is not a passive running gait, the amount of the control is very small. Figure 9 shows that the energy dissipation coefficient  $\mu^-$  in Eq. (28) eventually converges to zero. It implies that the condition (29) is achieved and there is no energy dissipation at the touchdown. Finally, Fig. 10 exhibits that the phase portraits of  $q-\dot{q}$  of the resultant gait forms a closed orbit. From those figures, the gait transition to an optimal periodic gait with respect to the energy consumption is achieved.

## 5 Conclusion

In this paper, both the control input and some adjustable plant parameters have been simultaneously optimized, by utilizing optimal learning control based on variational symmetry of Hamiltonian systems. We have extended the method in [20] so as to enable to optimize the plant parameters within a prescribed range by applying the input saturation technique of ILC [4] to a virtual input induced from an adjustable parameter to be optimized. In this framework, the robot keeps walking and the gait is optimized with respect to the energy consumption. We have respectively applied the proposed method to the passive walking and running robots. In the first case, the gait transition to a passive walking is achieved as an optimal solution by simultaneously optimizing the control input and the mass distribution of the leg. In the second case, an optimal periodic gait with respect to the energy consumption is achieved by simultaneously optimizing the control input and the hip spring stiffness. The proposed method has advantages that optimality of the resultant trajectory is guaranteed and the precise model of the dynamics is not required.

## References

- Ahmadi, M., Buehler, M.: Stable control of a simulated one-legged running robot with hip and leg compliance. *IEEE Trans. Robotics and Automation* **13**(1), 96–104 (1997)
- Asano, F., Luo, Z.W.: Energy-efficient and high-speed dynamic biped locomotion based on principle of parametric excitation. *IEEE Trans. Robotics* **24**(6), 1289–1301 (2008)
- Asano, F., Yamakita, M., Kamamichi, N., Luo, Z.W.: A novel gait generation for biped walking robots based on mechanical energy constraint. *IEEE Trans. Robotics and Automation* **20**(3), 565–573 (2004)
- Fujimoto, K., Horiuchi, T., Sugie, T.: Optimal control of Hamiltonian systems with input constraints via iterative learning. In: Proc. 42nd IEEE Conf. on Decision and Control, pp. 4387–4392 (2003)
- Fujimoto, K., Koyama, I.: Iterative feedback tuning for Hamiltonian systems. In: Proc. 17th IFAC World Congress, pp. 15,678–15,683 (2008)
- Fujimoto, K., Sugie, T.: Canonical transformation and stabilization of generalized Hamiltonian systems. *Systems & Control Letters* **42**(3), 217–227 (2001)
- Fujimoto, K., Sugie, T.: Iterative learning control of Hamiltonian systems: I/O based optimal control approach. *IEEE Trans. Autom. Contr.* **48**(10), 1756–1761 (2003)
- Garcia, M., Chatterjee, A., Ruina, A., Coleman, M.: The simplest walking model: Stability, complexity, and scaling. *ASME J. Biomechanical Eng.* **120**, 281–288 (1998)
- Goswami, A., Espiau, B., Keramane, A.: Limit cycles in a passive compass gait biped and passivity-mimicking control laws. *Autonomous Robots* **4**(3), 273–286 (1997)
- Goswami, A., Thuilot, B., Espiau, B.: Compass-like biped robot part i: Stability and bifurcation of passive gaits. INRIA Research Report (2996) (1996)
- Grizzle, J.W., Abba, G., Plestan, F.: Asymptotically stable walking for biped robots: analysis via systems with impulse effects. *IEEE Trans. Autom. Contr.* **46**(1), 51–64 (2001)
- Hyon, S.: Hamiltonian-based running control of dynamic legged robots. *Systems, Control and Information* **49**(7), 260–265 (2005). (in Japanese)
- Hyon, S., Emura, T.: Energy-preserving control of passive one-legged running robot. *Advanced Robotics* **18**(4), 357–381 (2004)
- Hyon, S., Emura, T.: Symmetric walking control: Invariance and global stability. In: Proc. IEEE ICRA, pp. 1455–1462 (2005)
- McGeer, T.: Passive dynamic walking. *Int. J. Robotics Research* **9**(2), 62–82 (1990)
- Osuka, K., Kirihara, K.: Motion analysis and experiments of passive walking robot QUARTET II. In: Proc. IEEE Int. Conf. Robotics and Automation, pp. 3052–3056 (2000)
- Sano, A., Ikemata, Y., Fujimoto, H.: Analysis of dynamics of passive walking from storage energy and supply rate. In: Proc. IEEE Int. Conf. Robotics and Automation, pp. 2478–2483 (2003)
- Satoh, S., Fujimoto, K., Hyon, S.: Gait generation for passive running via iterative learning control. In: Proc. IEEE/RSJ Int. Conf. Intelligent Robots and Systems, pp. 5907–5912 (2006)
- Satoh, S., Fujimoto, K., Hyon, S.: Biped gait generation via iterative learning control including discrete state transitions. In: Proc. 17th IFAC World Congress, pp. 1729–1734 (2008)
- Satoh, S., Fujimoto, K., Hyon, S.: Gait generation via unified learning optimal control of Hamiltonian systems. *Robotica* **31**(5), 717–732 (2013)
- Satoh, S., Fujimoto, K., Saeki, M.: Input and plant parameter optimization via learning optimal control of Hamiltonian systems. In: Proc. IFAC 5th Workshop on Lagrangian and Hamiltonian Methods for Nonlinear Control, p. (USB) 0043 (2015)
- Spong, M.W.: Passivity based control of the compass gait biped. In: Proc. of IFAC World Congress, pp. 19–23 (1999)
- Thompson, C., Raibert, M.: Passive dynamic running. In: V. Hayward, O. khatib (eds.) *Experimental Robotics I, Lecture Notes in Control and Information Science*, vol. 139, pp. 74–83. Springer-Verlag, Berlin (1989)